










## RESEARCH ARTICLE

WILEY

# Depression recurrence is accompanied by longer periods in default mode and more frequent attentional and reward processing dynamic brain-states during resting-state activity

Sonsoles Alonso<sup>1,2</sup>  | Anna Tyborowska<sup>3,4</sup>  | Nessa Ikani<sup>3,5,6</sup>  |  
 Roel J. T. Mocking<sup>7</sup>  | Caroline A. Figueroa<sup>8,9</sup>  | Aart H. Schene<sup>3,4†</sup> |  
 Gustavo Deco<sup>10,11</sup>  | Morten L. Kringelbach<sup>12,13,14</sup>  | Joana Cabral<sup>12,15</sup>  |  
 Henricus G. Ruhé<sup>3,4</sup> 

**Correspondence**

Sonsoles Alonso, Department of Clinical Medicine, Centre of Functionally Integrative Neuroscience, Aarhus University, Aarhus, Denmark.

Email: [sonsoles.alonso@cfni.au.dk](mailto:sonsoles.alonso@cfni.au.dk)

Anna Tyborowska, Department of Clinical Psychology, Behavioural Science Institute, Radboud University, Nijmegen, the Netherlands.

Email: [anna.tyborowska@donders.ru.nl](mailto:anna.tyborowska@donders.ru.nl)

**Funding information**

Academisch Medisch Centrum, AMC MD-PhD Scholarship, AMC PhD Scholarship, Amsterdam UMC Starter Grant; Carlsbergfondet; Danmarks Grundforskningsfond, Grant/Award Number: DNR117; Fundação para a Ciência e a Tecnologia, Grant/Award Numbers: UIDB/50026/2020, UIDP/50026/2020; Hersenstichting, Grant/Award Numbers: 2009 (2)-72, HA2015.01.07; 'la Caixa' Foundation, Grant/Award Number: LCF/BQ/PR22/11920014; Nederlandse Organisatie voor Wetenschappelijk Onderzoek, Grant/Award Number: Veni 016.126.059; Pettit Foundation; Universiteit van Amsterdam, ABC Talent Grant; ZonMw GGZ fellowship

**Abstract**

Recurrence in major depressive disorder (MDD) is common, but neurobiological models capturing vulnerability for recurrences are scarce. Disturbances in multiple resting-state networks have been linked to MDD, but most approaches focus on stable (vs. dynamic) network characteristics. We investigated how the brain's dynamical repertoire changes after patients transition from remission to recurrence of a new depressive episode. Sixty two drug-free, MDD-patients with  $\geq 2$  episodes underwent a baseline resting-state fMRI scan when in remission. Over 30-months follow-up, 11 patients with a recurrence and 17 matched-remitted MDD-patients without a recurrence underwent a second fMRI scan. Recurrent patterns of functional connectivity were characterized by applying Leading Eigenvector Dynamics Analysis (LEIDA). Differences between baseline and follow-up were identified for the 11 non-remitted patients, while data from the 17 matched-remitted patients was used as a validation dataset. After the transition into a depressive state, basal ganglia-anterior cingulate cortex (ACC) and visuo-attentional networks were detected significantly more often, whereas default mode network activity was found to have a longer duration. Additionally, the fMRI signal in the basal ganglia-ACC areas underlying the reward network, were significantly less synchronized with the rest of the brain after recurrence (compared to a state of remission). No significant changes were observed in the matched-remitted patients who were scanned twice while in remission. These findings characterize changes that may be associated with the transition from remission to recurrence and provide initial evidence of altered dynamical exploration of the brain's repertoire of functional networks when a recurrent depressive episode occurs.

Sonsoles Alonso and Anna Tyborowska shared first authorship.

† Deceased.

For affiliations refer to page 5780

This is an open access article under the terms of the [Creative Commons Attribution](https://creativecommons.org/licenses/by/4.0/) License, which permits use, distribution and reproduction in any medium, provided the original work is properly cited.

© 2023 The Authors. *Human Brain Mapping* published by Wiley Periodicals LLC.

## KEYWORDS

dynamic functional connectivity, MDD, recurrence, resting-state fMRI

## 1 | INTRODUCTION

Major Depressive Disorder (MDD) is a severe and highly prevalent disease affecting 5% of the global population (Institute of Health Metrics and Evaluation, 2019). An important factor in the high personal and societal impact of MDD is the high risk of recurrence (Bockting et al., 2009; Hardeveld et al., 2010). Nevertheless, neurobiological investigations of the recurrence of depressive episodes remain scarce. This study addresses the critical issue of how network dynamics change when patients transition from a remitted to a recurrent depressed state.

MDD has been associated with disturbances in multiple resting-state networks, including the default mode network (DMN), salience and frontal networks—regulating cognitive control and attention (Kaiser et al., 2015; Menon, 2011; Mulders et al., 2015). Recent studies have further shown that MDD may be related to alterations in large-scale functional connectivity (FC) between these networks (Li et al., 2020; Liu et al., 2020). Specifically in remitted depressed patients, functional hyper-connectivity in, for example, DMN and dorsal attention network, as well as within and between salience and executive control networks have been reported (Liu et al., 2021).

The majority of research conducted in MDD has largely focused on discerning differences between patients and healthy controls or predicting vulnerability for relapse from baseline assessments. In this respect, dominance of activity within the DMN has been associated with MDD recurrence and related to rumination (Lythe et al., 2015; Marchetti et al., 2012), whilst decreased within network FC of the DMN has been shown to predict more depressive symptoms within a 2-year follow-up period (Blank et al., 2021). Another study points to the neuro-progressive nature of MDD, with remitted depressed patients (compared to first episode patients) showing hyper-connectivity in a wide range of networks, including the DMN (Liu et al., 2021). However, a within-subject investigation of changes in large-scale FC during the transition into a depressive episode, to our knowledge, has never been investigated.

A recent meta-analysis suggests limited convergence of findings across resting-state measures (Gray et al., 2020), despite previous reports to the contrary (Kaiser et al., 2015). One of the reasons for heterogeneity in findings may be related to the fact that studies thus far have primarily applied static resting state measures, which capture only the stable dimensions of FC, without addressing processes by which regions in the brain integrate in networks, which interact with other networks and dissolve over time. Recent insights, however, support indices of the alteration of brain network connectivity over time as potential markers for affective disorders, which might provide insights into altered neural communication in MDD (Figueroa et al., 2019; Kaiser et al., 2016). It is, therefore, crucial to use a dynamic approach that assesses the integration and segregation

(Deco et al., 2015) of time-varying neurocognitive brain networks (Barrett & Satpute, 2013; Bressler & Menon, 2010; Deco & Kringelbach, 2014; Yarkoni et al., 2011) in order to adequately capture the neural correlates of MDD and its recurrence.

A promising avenue in this regard is dynamic FC, based on growing evidence that neural activity at rest is not stable, but slowly fluctuates through varying, but repeating states (Cabral et al., 2017). For example, a recent study in MDD patients has shown disrupted organization of dynamic brain networks with respect to higher variability and lower consistency in FC between time-points, as compared to healthy controls (Long et al., 2020).

A novel method for investigating dynamic FC is Leading Eigenvector Dynamics Analysis (LEIDA), which identifies whole-brain phase-locking (PL) patterns in fMRI signals at every time-point, that are clustered into repeating FC states (Cabral et al., 2017). Each FC state reveals synchronization within a specific set of brain areas and is characterized by its probability of occurrence (fractional occupancy) and duration (lifetime). In comparison to other analytical tools, LEIDA extends from measures of connectivity or correlation by considering also the phase-shifts between brain regions and describes discrete instead of overlapping states in time (Kringelbach & Deco, 2020). Dynamic characteristics of FC states derived from LEIDA have been related to cognitive performance (Cabral et al., 2017), emotionality (Stark et al., 2020), depressive symptoms (Alonso Martínez et al., 2020), trait self-reflectiveness (Larabi et al., 2020), body dysmorphic disorder (Wong et al., 2021), schizophrenia (Farinha et al., 2022), and distinct mood states in remitted MDD (rMDD) patients (Figueroa et al., 2019), which reinforces its sensitivity to both clinical and pre-clinical psychiatric symptoms.

The goal of this study was to investigate how dynamic FC states change when patients shift from remission to recurrence of a new depressive episode. We hypothesized that patients experiencing a recurring depressive episode would show changes in fractional occupancy and lifetime of FC states of DMN, attentional, and salience networks, compared to a remitted state.

## 2 | MATERIALS AND METHODS

### 2.1 | Participants

As part of a larger project investigating the neurobiology of recurrence of depressive episodes (Mocking et al., 2016), 62 drug-free (>4 weeks), rMDD patients (age 35–65 years) with  $\geq 2$  episodes (according to the Structured Clinical Interview for DSM-IV Disorders [SCID]), underwent a baseline resting-state fMRI scan when in remission (Hamilton Depression Rating Scale [HDRS-17] score  $\leq 7$  for  $\geq 8$  weeks). Exclusion criteria were alcohol/drug dependency;

**TABLE 1** Sample characteristics.

	Non-recurrent ( <i>n</i> = 17)	Recurrent ( <i>n</i> = 11)	
Sex			
Women	13	9	<i>p</i> = 1 <sup>a</sup>
Men	4	2	
Age	53.5 (6.9)	50.5 (5.75)	<i>t</i> (26) = 1.23
IQ	107 (9.21) <sup>b</sup>	108 (8.04) <sup>c</sup>	<i>t</i> (23) = .084
Episodes in the past (number)	6.76 (11.8)	11.40 (18) <sup>c</sup>	<i>U</i> = 108
Months since baseline	11.6 (5.86)	10.2 (6.27)	<i>t</i> (26) = .601
Completed FU time-point at second MRI	2.18 (1.38)	2.45 (1.57)	<i>U</i> = 106
HDRS baseline	3.69 (2.85)	6.11 (5.49)	<i>U</i> = 117
HDRS at second MRI	3.73 (3.64)	20.4 (5.38)	<i>U</i> = 185**

Note: Values indicate the mean and standard deviation.

Abbreviations: FU, follow-up; HDRS, Hamilton Depression Rating Scale.

<sup>a</sup>Fisher's exact test.

<sup>b</sup>*n* = 15.

<sup>c</sup>*n* = 10.

\*\**p* < .001.

psychotic or bipolar disorder; predominant anxiety disorder or severe personality disorder; electroconvulsive therapy within 2 months before scanning and current severe physical illness. MRI exclusion criteria were: incompatible implants or tattoos, claustrophobia, history of seizure or head injury, and neurological disorder. Participants were recruited from primary care, secondary mental health-care institutes, from previous studies, and through advertisements in online and house-to-house newspapers and posters in public places.

Over a 30-month follow-up period, a second fMRI scan was obtained from patients reporting a recurrence. Follow-up assessments of the rMDD participants were conducted by phone at regular intervals (every~4 months), during which the SCID and HDRS were administered. To maximize the detection rate of recurrences, participants were also instructed to contact the study researchers if they subjectively experienced a recurrence. Overall, 55% of patients had a recurrence (based on SCID criteria). Of these, in 11 patients, we were able to capture the recurrent depressive episode in time and motivate the patient for a second scan during the depressive episode. Seventeen rMDD-patients without a recurrence; matched for age, sex, IQ, and length of follow-up were also scanned a second time (Table 1). For more information on the full sample and recurrence rates, see Figueira et al. (2019) and Ruhe et al. (2019). Informed consent was obtained prior to participation; the study was approved by the local Medical Ethical Committee of Amsterdam UMC. Clinical registration of the study was done in the Dutch National Trial Register (trial number: NTR3768).

## 2.2 | Image acquisition

A 3 Tesla Philips Achieva XT scanner (Philips Medical Systems, Best, the Netherlands), with a 32-channel SENSE head coil, was used to obtain the images. A high-resolution T1-weighted 3D structural image was acquired using fast-field echo (FFE) for anatomical reference

(220 slices; TR: 8.3 ms; TE: 3.8 ms; FOV: 240 × 188; 240 × 240 matrix; voxel size: 1 × 1 × 1 mm). Functional images were acquired with a T2\*-weighted gradient echo-planar imaging (EPI) sequence. Participants were instructed to close their eyes and stay awake. The scan comprised 208 volumes of 37 axial-slices (TR: 2000 ms; TE: 27.6 ms; FOV: 240 × 240; 80 × 80 matrix; voxel size: 3 × 3 × 3 mm), oriented parallel to the AC-PC transverse plane and acquired in ascending order with a gap of 0.3 mm.

## 2.3 | Image preprocessing and analysis

### 2.3.1 | Image preprocessing

fMRI data were preprocessed using FSL version 6.0 (FMRIB, Oxford, UK). To control for T2\* equilibration effects, the first four volumes were discarded. Images were aligned to the first scan using rigid body transformations, spatially smoothed with a 5-mm FWHM Gaussian kernel, grand-mean intensity normalization by a single multiplicative factor, and denoised using a non-aggressive ICA-AROMA procedure (Pruim et al., 2015). Model nuisance effects were regressed out from the preprocessed images with a linear model. These included 24 head-motion parameters: 6 motion regressors, their derivatives, and squared terms of each (Caballero-Gaudes & Reynolds, 2017; Friston et al., 1996). Brain extraction of T1 images was performed using the FSL anat preprocessing tool, resulting in bias-corrected images, subsequently segmented into white matter and CSF. Subject-specific white matter and CSF masks were thresholded at 95% probability and coregistered to the functional images. Mean signal intensities were extracted per volume and regressed from the preprocessed fMRI images along with the motion regressors. High pass filtering with a cut-off of 100 s was performed on the residual images from the linear model. Images were normalized to the Montreal Neurological Institute template (MNI152) using linear (FLIRT; Jenkinson

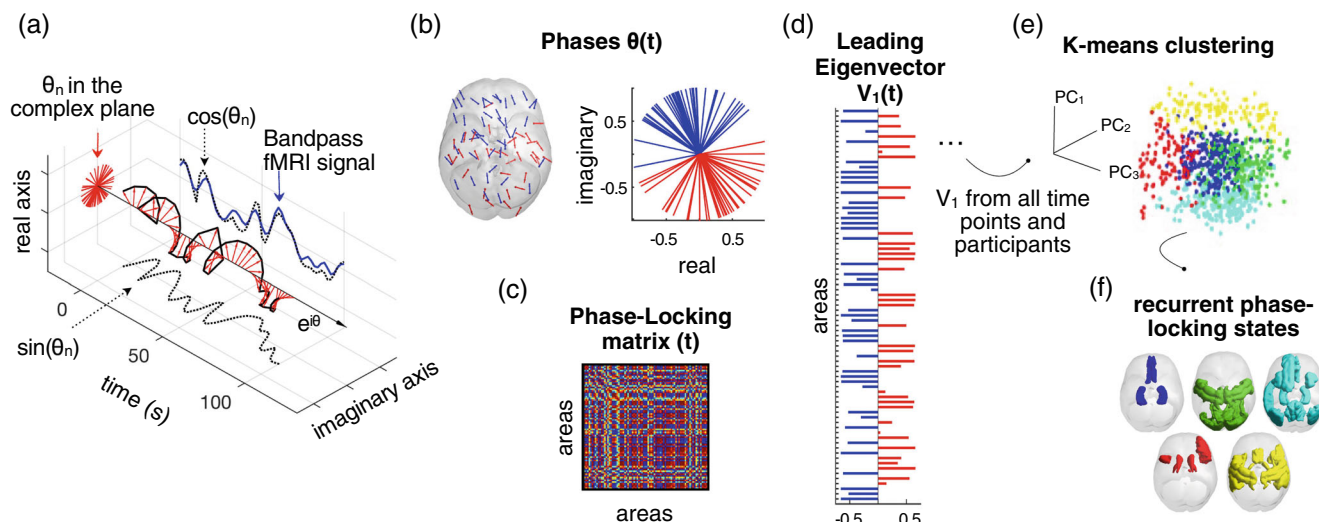


**FIGURE 1** Detection of recurrent phase-locking (PL) patterns in fMRI signals. (a) The fMRI signal is band-pass filtered between 0.01 and 0.1 Hz (blue) and Hilbert transformed into an analytic signal, whose phase can be represented over time ( $e^{i\theta}$  black arrow) and at each TR (red arrows). (b) The phases in all  $N = 80$  regions at a single TR are represented in the complex plane (right) and cortical space (left; arrows are placed at the center of gravity of each region  $n$ ; the direction and color of the arrows indicate the sign of the corresponding element in the leading eigenvector  $V_1(n,t)$  (red for positive and blue for negative). (c) The PL matrix captures the phase alignment between each pair of regions. (d) The leading eigenvector of the PL matrix at time  $t$ ,  $V_1(t)$  captures the main orientation of all phases. (e) The leading eigenvectors obtained for each time point are concatenated over scans and subjects, and fed into a k-means clustering algorithm which divides the pool of data points into a predefined number of clusters  $k$ . (f) Cortical representation of the PL-states (clusters). PL = phase-locking (right).

et al., 2002; Jenkinson & Smith, 2001) and nonlinear (FNIRT; Andersson et al., 2007) transformations via boundary-based registration (BBR; Greve & Fischl, 2009).

Time series were extracted using an 80-region Mindboggle-modified parcellation, following Deco et al. (2021). The Desikan–Killiany–Tourville (DKT) labeling protocol (Desikan et al., 2006) was used to parcellate each cortical hemisphere into 31 anatomical regions. Additionally, nine subcortical regions were added for each hemisphere: hippocampus, amygdala, subthalamic nucleus, globus pallidus internal segment, globus pallidus external segment, putamen, caudate, nucleus accumbens, and thalamus. The FSL function, `fslmeants`, was used to calculate an average over voxels within each ROI to get the representative time courses. Finally, temporal band-pass filtering was applied to detrend the time course signal and to retain frequencies between 0.01 and 0.1 Hz.

### 2.3.2 | Leading Eigenvector Dynamics Analysis

We applied LEIDA to characterize recurrent PL patterns in fMRI signals. This data-driven approach relies on the leading eigenvector of the phase coherence matrix at each single TR (Cabral et al., 2017). First, participant-specific sets of 80 ROI time courses were demeaned and Hilbert transformed to estimate the phase of the ROI signals (Figure 1a). The Hilbert transform expresses any given signal  $x$  in polar coordinates, that is,  $x = A \cos \theta$ , where  $A$  is the instantaneous amplitude, and  $\theta$  the instantaneous phase at a given time point. Then, at each time point, the phase coherence between two regions,  $n$  and  $p$ ,

can be calculated as the cosine of the phase differences as in the following equation:

$$PL(n,p) = \cos(\theta(n) - \theta(p))$$

where PL takes values from 1 to  $-1$ , for signals changing in the same or opposite direction, respectively (Figure 1b). This process results in a time-resolved dynamic phase-locking (dPL) matrix with size  $N \times N \times T$ , where  $N$  ( $=80$ ) is the number of brain regions and  $T$  ( $=204$ ) is the number of recording frames in each scan (Figure 1c). The first and last volumes of each scan were removed to account for boundary distortions associated with the Hilbert transform. Next, the leading eigenvector,  $V_1$ , of each PL matrix was calculated (Figure 1d). The leading eigenvector captures the dominant instantaneous connectivity pattern, which substantially reduces data dimensionality from  $N \times N$  to  $N \times 1$ .

### 2.3.3 | Detection and characterization of recurrent PL-states

We employed a data mining approach that successively partitions the data searching for the partitions that are able to detect changes associated with the recurrence of a new MDD episode. Although an open question in dynamic FC research is the number of recurrent brain states, here we do not aim to identify the optimal number of PL-states explored during resting-state activity. Instead, we aimed to identify and characterize the dynamics of recurrent FC patterns that could

potentially explain changes associated with the experience of a new depressive episode. As brain signatures related to MDD recurrence may arise at different levels of granularity, we used a  $k$ -means clustering algorithm, which was run for 19 partition models by varying the number of clusters  $k$  from 2 to 20, with higher  $k$  resulting in more fine-grained configurations. For each  $k$ , the 4488 leading eigenvectors (resulting from 11 subjects, 2 scans, 204 volumes each) were partitioned into  $k$  clusters (Figure 1e), resulting in  $k$  cluster centroids of  $N \times 1$  dimensions, each representing a recurrent PL-state (Figure 1f). With the PL-states derived from the data of the 11 recurring patients, we applied these to the 17 matched nonrecurring, remitted patients used for the validation step. In these 17 nonrecurring rMDD patients, 6936 leading eigenvectors were obtained (17 subjects, 2 scans, 204 volumes); a  $k$ -means clustering with a single iteration, using the cluster centroids from the recurring group as “start vectors” defining identical PL-states.

PL-states were characterized according to their fractional occupancy and lifetime. Fractional occupancy is calculated as the temporal proportion of epochs assigned to a given cluster centroid, that is, the proportion of time in which a PL-state was active. The lifetime of each PL-state is the mean number of consecutive epochs in the same state.

### 2.3.4 | Phase-shifted signals between brain regions

Previous studies show that LEiDA captures relevant phase-shifts between brain regions (e.g., Cabral et al., 2017; Figueroa et al., 2019), which is often missed with typical measures of correlation. Phase locking is a measure of synchronization that preserves both in-phase and anti-phase relationships in the data (Hancock et al., 2022). To further investigate the relevance of signals that are shifted in phase, we obtained a “decoupling metric”—calculated as a continuous metric to estimate the phase shift of a given functional subsystem from the rest of the brain. Since each PL-state is represented by a  $N \times 1$  vector with positive and negative elements, we calculated the mean phase across regions with a positive sign and the mean phase across regions with a negative sign, and then calculated the angular difference between these two phase signals over time—obtaining a temporal signature capturing the degree of shift between the functional network detected in each PL-state and the rest of the brain. We averaged the angular difference over time for a metric of total phase shifting of a given functional network that can be compared between scan-sessions or subjects. The moments when segregation or “decoupling” is observed can be considered the activation of the given functional network—not in sync with the rest of the brain.

## 2.4 | Statistical analysis

Given the moderate number of patients involved, a repeated measures ANOVA investigating the group-by-time interaction was not justified. Therefore, differences in fractional occupancy and lifetime were statistically assessed between scans in the recurring group

separately, using a nonparametric permutation-based paired  $t$ -test (5000 permutations). In line with Figueroa et al. (2019),  $p$ -values were adjusted for each of the 19 partition models obtained by  $k$ -means clustering by controlling the false discovery rate (FDR) as proposed by Benjamini and Hochberg (1995).

As indicated above, with the PL-states identified in recurring patients, we repeated the analyses in the matched nonrecurring rMDD patients, as a validation of the specificity of findings. Moreover, in a sensitivity analysis, we determined the re-occurrence of PL-states in the nonrecurring rMDD patients separately. Therefore, the  $k$ -means clustering was applied directly on the 6936 leading eigenvectors from the nonrecurring patients (from 17-subjects, 2-scans, 204-volumes), and the two sessions were compared using a nonparametric permutation-based paired  $t$ -test (5000 permutations) for fractional occupancy and lifetime.

In the identified PL-states, post-hoc, we compared the decoupling metric between the two sessions. Again, we used permutation paired  $t$ -tests in the recurring and nonrecurring group separately.

In a post-hoc analysis, we used Bayesian paired  $t$ -tests to quantify evidence in favor of the alternative hypothesis (recurring patients) and in favor of the null hypothesis (nonrecurring patients) in the states identified with the above-described frequentist approach.

## 3 | RESULTS

Recurring and nonrecurring patients did not differ with respect to number of men/women, age, IQ, number of depressive episodes, months since baseline assessment, and follow-up time-point of the second MRI session. The groups were matched on HDRS scores at baseline, but as expected, differed on their HDRS scores during the follow-up scan, with recurrent patients having a significantly higher symptom score. See Table 1 for sample characteristics and statistics. Patients who were scanned did not differ from the overall sample that had a recurrence during the follow-up period (Supplementary Material Table S3).

### 3.1 | Recurrence-related changes in PL-state fractional occupancy

Significant differences in fractional occupancy between baseline and follow-up occurred in states characterized by fine-grained network configurations (Figure 2). Partition  $k = 18$  was the first partition model to return significant changes associated with the recurrence of a new MDD episode. Specifically, the average fractional occupancy of two states increased from remission to recurrence: PL-state k18c10 ( $t(10) = 2.91$ ;  $p$ -FDR = .039,  $d = .88$ ), which comprises areas of the reward system, namely, basal ganglia and anterior cingulate cortex (ACC), and k18c15, ( $t(10) = 3.14$ ;  $p = .004$ ;  $p$ -FDR = .039,  $d = .95$ ), which includes connections of the visual and dorsal attention network (Figure 2c). These two PL-states (i.e., clusters c10 and c15 for  $k = 18$ ) are represented in Figure 2b as vectors, where each



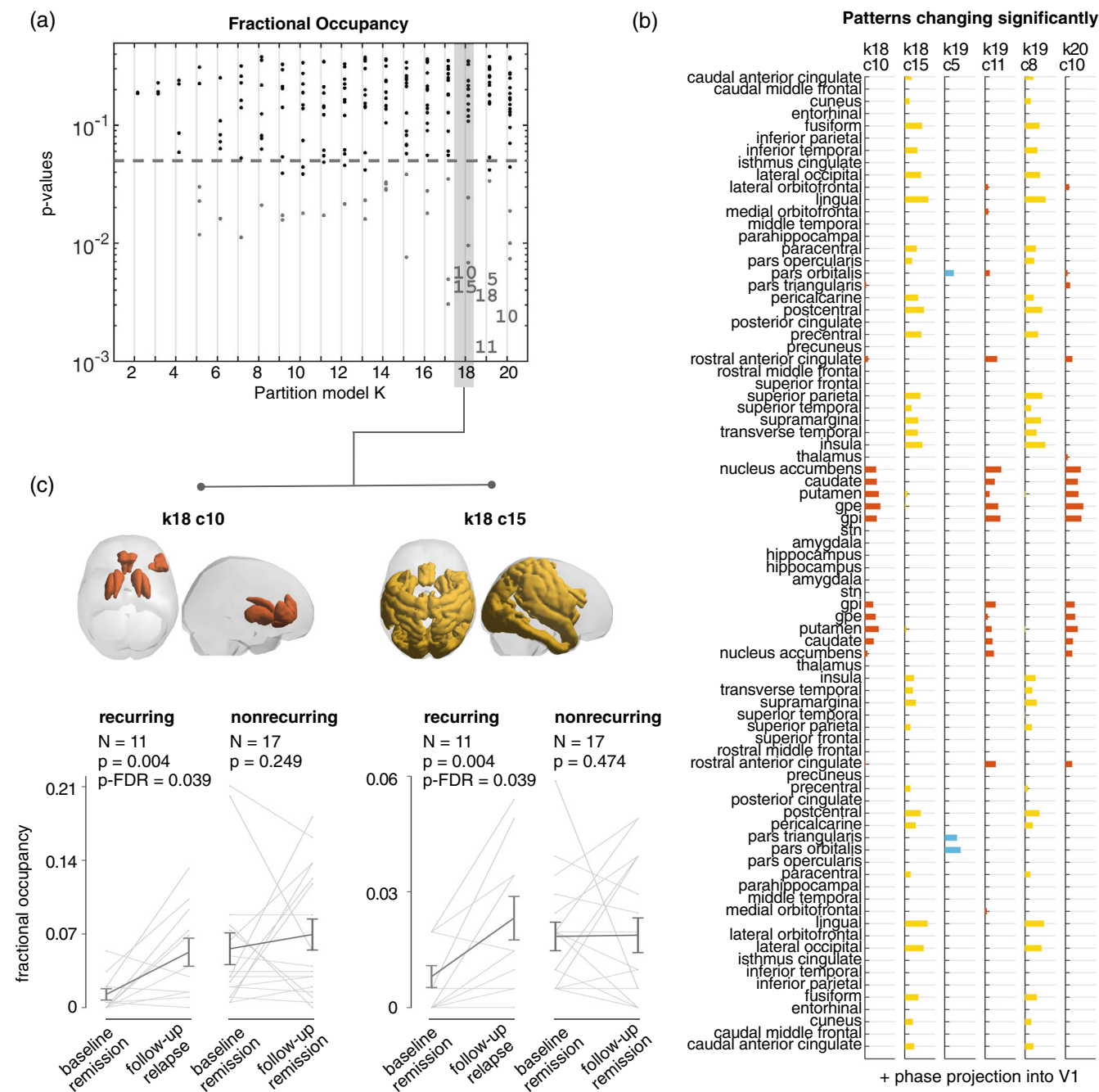


**FIGURE 2** Significant increases in the fractional occupancy of two PL-states during the experience of a new MDD episode. (a) Statistical significance associated with changes in fractional occupancy from remission to recurrence, in the entire repertoire of PL-states returned by each of the 19 partition models (k2–k20). While most PL-states do not show significant changes (black dots) between baseline (remission) and follow-up (recurrence), for all  $k > 17$ , two PL-states repeatedly survive FDR corrections (indicated with numbers). PL-states failing to reach the FDR-corrected significance threshold but with  $p_{\text{uncorrected}} < 0.05$  are indicated with gray dots. PL-states are labeled from 1 to  $k$  number of clusters considered in each partition model; as a result, variant forms of the same underlying PL-state do not necessarily have the same label in every partition. (b) Vector representation of the PL-states with a significant ( $p\text{-FDR} < .05$ ) change in their fractional occupancy from baseline (remission) to follow-up (recurrence). Each bar plot shows the elements in V1, representing fMRI signals of brain regions that become coherent and phase-shifted by more than  $90^\circ$  with respect to the signals in the rest of the brain. States are color-coded according to their similarities; similar forms of these two states also appear in partition k19 and k20 (and also in higher partitions see Supplementary Material Figure S1 for partitions up to k30). (c) Cortical space representation of the two PL-states, only rendering regions where the phase is shifted more than  $90^\circ$  with respect to the main phase orientation. Underneath each brain plot, graphical representation of the changes in fractional occupancy between baseline and follow-up for the recurring rrMDD patients (i.e., recurrence at follow-up) and the nonrecurring rrMDD patients (i.e., maintaining remission at follow-up). Gray lines represent patient-specific scores, and error-bars represent the mean  $\pm$  standard error of the mean across subjects. PL = phase-locking.

element represents a brain area, and whose value indicates the degree to which the signal in these areas shifts from the main phase direction.

Significance and effect-sizes were comparable for the  $k = 19$  and 20 clustering solutions. Validating the specificity of our findings in recurring rMDD-patients, we verified that the fractional occupancy of these two states did not significantly change in nonrecurring rMDD-patients. Supplementary Material Table S1 shows the fractional occupancy scores and statistics for all PL-states in partition  $k = 18$ .

Finally, post-hoc Bayesian paired  $t$ -tests showed moderate evidence for the alternative hypothesis (baseline < follow-up) in the reward network (basal ganglia, ACC; Bayes Factor = 8.34) and strong evidence in the visual-attention network (Bayes Factor = 11.45) in recurring patients. In nonrecurring patients, there was moderate evidence in favor of the null hypotheses (no difference between baseline and follow-up) in the reward network (basal ganglia, ACC; Bayes Factor = 3.21) and visual-attention network (Bayes Factor = 4.01).

### 3.2 | Recurrence-related changes in state lifetime

We also explored within-subject differences regarding state lifetime, which is the duration (in seconds) that a given state occurs. We found two distinct states that significantly changed from baseline to follow-up for several partition models (Figure 3a). At lower numbers of PL-state partitions ( $k = 3, 4, 6$ ), a PL-state (k3c3) that consisted of the DMN showed significantly longer lifetimes (shown in gray in Figure 3b). Partitioning the data into a high number of clusters ( $k > 8$ ) returned a state characterized by connections within the reward network (shown in brown in Figure 3b; k8c4, k10c5, k11c5, k14c7, k17c8, k19c11, k20c10); a variant form of this state was also found to be significantly different from remission to recurrence in terms of fractional occupancy.

The lifetime of a state is calculated as the average number of consecutive frames in that state. The higher the number of clusters considered in a partition model, the shorter the state lifetimes. Given the relatively short length of the recording session (204 volumes) with a TR of 2 s, the states resulting from partitions with higher cluster numbers should be interpreted with caution. Therefore, here, we focused on the state returned by the lowest partition: PL-state 3 (k3c3). As Figure 3c shows, the mean lifetime of PL-state k3c3 significantly increased from remission to recurrence ( $t(10) = 2.44$ ;  $p$ -FDR = .038,  $d = .74$ ). Significance and effect-sizes were comparable for the  $k = 4$  and 6 clustering solutions.

Validating the specificity of our findings in recurring rMDD-patients, we did not find a significant difference in the lifetime of PL-state k3c3 for patients who were not experiencing a recurrent episode at follow-up ( $t(16) = .96$ ;  $p = .172$ ). Supplementary Material Table S2 shows the lifetime scores and statistics for the states in partition  $k = 3$ .

Post-hoc Bayesian paired  $t$ -tests showed moderate evidence for the alternative hypothesis (baseline < follow-up) in lifetime duration

of the DMN (Bayes Factor = 4.39) in recurring patients. In nonrecurring patients, there was relatively weak evidence in favor of the null hypotheses (no difference between baseline and follow-up) in the same network (Bayes Factor = 2.69).

### 3.3 | Phase shift of the reward system from the rest of the brain

To further investigate the effects captured with LEiDA, we analyzed how fMRI signals evolve over time in one of the subsystems found to “shift in phase” or “decouple” from the rest of the brain, significantly more often in rMDD-patients experiencing a recurrence relative to baseline. When PL-state k18c10 is on, signals in the regions with a positive sign in this PL-state (corresponding to the basal ganglia and ACC) align together and shift in phase with respect to regions with a negative sign (Figure 4a). When comparing the average phase shift between signals in the reward system (basal ganglia, ACC) and the rest of the brain, a significant increase in phase shift is detected when patients experienced a recurrence of MDD ( $t(10) = 2.65$ ,  $p = .008$ ; Figure 4b). Instead, no significant change was observed for patients who were still in remission at follow-up ( $t(16) = .14$ ,  $p = .446$ ). Supplementary Material Figure S2 illustrates in more detail the phase shift of the reward system from the rest of the brain.

### 3.4 | Sensitivity analysis

Since baseline–follow-up differences were tested on the PL-states that were defined solely from the two scan sessions of the recurring patients ( $n = 11$ ), we tested potential differences between baseline and follow-up on the states derived from the two scan sessions of the nonrecurring patients ( $n = 17$ ). The PL-states derived from this model resembled the PL-states as determined from the recurring patients (Supplementary Material Figure S3A). No significant ( $p$ -FDR < .05) differences were observed for any of the PL-states in any of the 19 partition models (k2–k20) between baseline (remission) and follow-up (maintained remission) for the matched nonrecurring patients (Supplementary Material Figure S3B).

## 4 | DISCUSSION

In the current study, we investigated dynamic FC changes that occurred in rMDD patients after transitioning from remission to a recurrence of a depressive episode. We found significant within-subject changes in the fractional occupancy and lifetime duration of three PL-states. Specifically, the basal ganglia–ACC circuit, part of the reward network, and a widespread visual-attention network were more likely to occur when suffering from a depressive episode as compared to being in a state of remission. Additionally, the DMN was activated for a longer duration during a recurrence of depression. As a

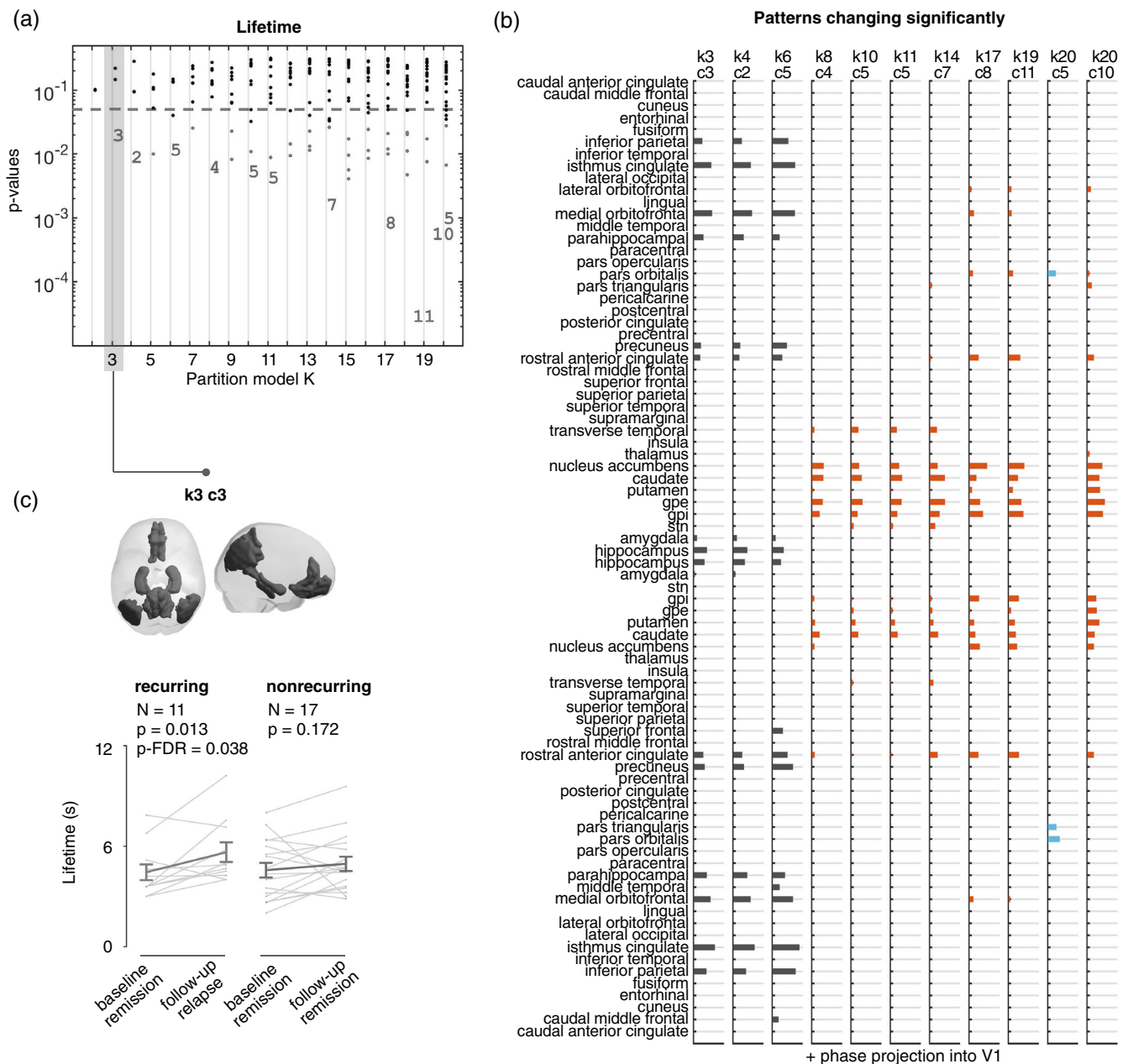


**FIGURE 3** Significant increase in PL-state 3 lifetime during the experience of a new MDD episode. (a) Statistical significance associated with changes in lifetime from remission to recurrence, in the entire repertoire of PL-states returned by each of the 19 partition models (k2–k20). While most PL-states do not show significant changes between remission and recurrence (black dots), two PL-states repeatedly survive FDR corrections (indicated with numbers). PL-states failing to reach the FDR-corrected significance threshold but with  $p_{\text{uncorrected}} < .05$  are indicated with gray dots. PL-states are labeled from 1 to k number of clusters considered in each partition model; as a result, variant forms of the same underlying PL-state do not necessarily have the same label in every partition. (b) Vector representation of the PL-states with a significant ( $p\text{-FDR} < .05$ ) change in their lifetime from baseline (remission) to follow-up (recurrence). Each bar plot shows the elements in V1, representing fMRI signals of brain regions that become coherent and phase-shifted by more than  $90^\circ$  with respect to the signals in the rest of the brain. States are color-coded according to their similarities. (c) Cortical space representation of the centroids of PL-state 3. Rendering only of regions phase-shifted more than  $90^\circ$  with respect to the fMRI signals in the rest of the brain. Underneath the brain plot, graphical representation of change in state lifetime between baseline and follow-up for the recurring rrMDD patients (i.e., recurrence at follow-up) and the nonrecurring rrMDD patients (i.e., maintaining remission at follow-up). Gray lines represent patient-specific scores, and error-bars represent the mean  $\pm$  standard error of the mean across subjects. PL = phase-locking.

validation, there were no statistically significant changes seen in a separate sample of matched rMDD patients scanned twice when remaining in remission with comparable follow-up times, age, sex, and

IQ. Finally, we showed post-hoc that the observed changes in the basal ganglia–ACC circuit, were due to an increased phase shift, that is “decoupling,” of this circuit from the rest of the brain.



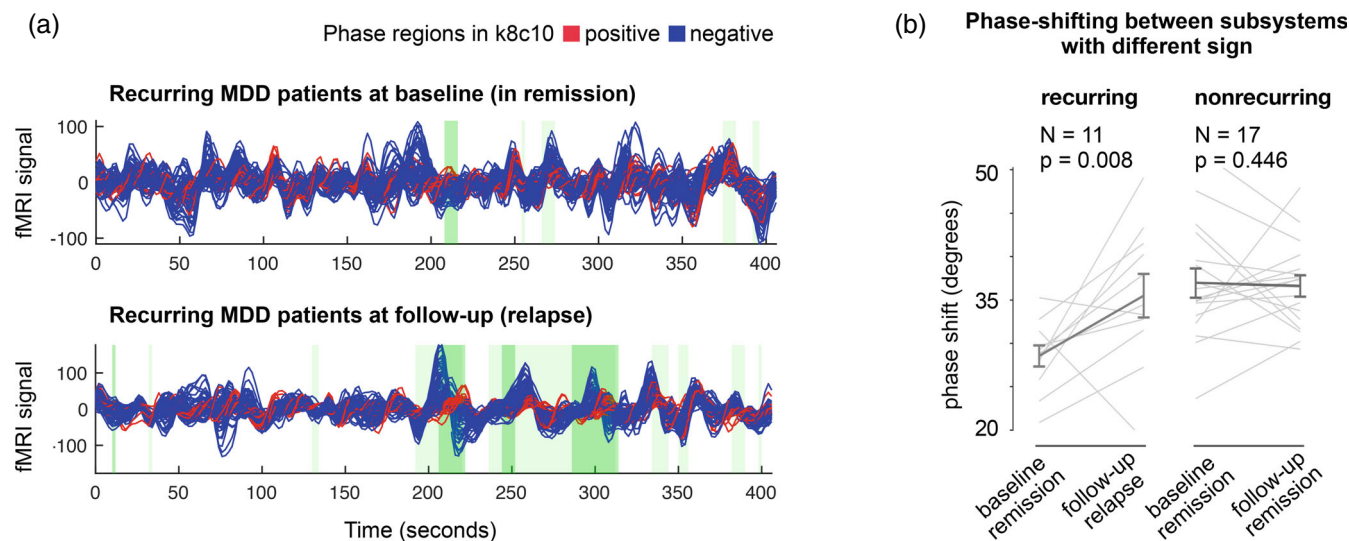


**FIGURE 4** Significant change in phase shift of the reward network from the rest of the brain during the recurrence of an MDD episode. (a) For illustrative purposes we visualize the fMRI signals in all 80 brain areas during remission (top) and at follow-up, when having a recurrence (bottom) in a single patient. Time-series of the positive community of k18c10 are shown in red, all the remaining brain regions are shown in blue. The three-dimensional effect is obtained by plotting the Hilbert-transformed ROI signals over time, but the view is shown only from one side. The signals have a real and an imaginary part, which can be perceived as a hidden dimension, on which they evolve while conserving angular momentum. The darker green patches indicate when the state k18c10 was detected by the k-means clustering. The lighter green patches indicate when the leading eigenvector  $V1(t)$  is relatively close to the centroid k18c10, to give a notion of when this state may be present, even if not dominant. (b) Evaluating the average phase-shift between regions of different signs in each PL-state (i.e., the red vs. the blue time series in panel (a)), we compare this measure across time points and conditions. The recurrent patients (i.e., recurrence at follow-up) are found to significantly increase the phase shift (in degrees) from baseline to follow-up, whereas the nonrecurrent rrMDD patients (i.e., maintaining remission at follow-up) do not exhibit any significant change. Gray lines represent patient-specific scores, and error-bars represent the mean  $\pm$  standard error of the mean across subjects. PL = phase-locking.

The striatum (caudate, putamen, nucleus accumbens) and ACC are main structures involved in different aspects of reward processing (Haber & Knudson, 2010) and part of the mesolimbic reward-circuitry underlying dopaminergic neurotransmission (Schott et al., 2008). Dysfunctions of prefrontal-basal ganglia/(para)limbic networks have been linked to a dysfunctional reward system in depressed patients (Martin-Soelch, 2009). In particular, hypo-activity of the striatum has been reported in MDD in reinforcement learning and reward processing task paradigms (Gradin et al., 2011; Hall et al., 2014; Kumar et al., 2008; Pizzagalli et al., 2009; Robinson et al., 2012; Smoski et al., 2009). Also in the overall sample of the DELTA-neuroimaging study, impaired learning signals in the ventral tegmental region differentiated rMDD patients and controls (Geugies et al., 2019), similar to Kumar et al. (2008).

Reward sensitivity has also been linked to differences in resting-state activity in the mesocortical pathway (Adrián-Ventura et al., 2019). Similar to task-based findings in MDD patients suggesting a deactivation of the reward system, FC measures report reduced coupling within prefrontal-basal ganglia circuits (caudate, putamen, nucleus accumbens) and link this to attenuated connectivity of the reward network (Li et al., 2018; Tol et al., 2013). This FC impairment has been related to depression severity and MDD symptoms (Satterthwaite et al., 2015; Zhu et al., 2017). In fact, this intrinsic FC

impairment appears to be progressive across the course of depression (Liu et al., 2021). Of note, others have shown that within the reward network, the ventral striatum exhibits both hyper- and hypo-connectivity (with the DMN) in MDD (Leaver et al., 2016) and increased information transfer between the OFC and subcortical (limbic) regions in first-episode MDD-patients (Gao et al., 2016). In line with these latter studies, we found increased fractional occupancy of a state comprised of regions subserving the reward network, namely the striatum/basal ganglia (caudate, putamen, nucleus accumbens) and ACC, whilst experiencing a depressive episode.

The ACC is not only involved in reward processes but has a broader role in the integration of attentional and affective information necessary for evaluative and regulatory processes (Etkin et al., 2011). Stemming from this, altered ACC functioning has been proposed as a key neural correlate of MDD (Davey et al., 2012; Hamilton et al., 2013; Kantrowitz et al., 2021). For example, a review by Rive et al. (2013) found that the ACC was both hyper- and hypo-active in MDD, depending on the type of task that was assessed. Other studies have shown aberrant resting-state connectivity of the ACC in MDD patients. For example, higher levels of depression were correlated with decreased connectivity between the ACC and precuneus in first-episode adolescents (Connolly et al., 2013) and less flexibility (i.e., fewer dynamic connectivity

changes) of the ACC in patients with MDD (Zheng et al., 2018). Changes in the fractional occupancy of the ACC (as part of a larger network state) during a depressive episode fits with its purported role in MDD neuropathology.

Note that the increased fractional occupancy of this state may not directly translate to increased activity or connectivity of a network. By introducing a new “decoupling metric,” we further demonstrated that this state was characterized by a consistent de-phasing of reward network areas from the rest of the brain, suggesting network decoupling and segregation during recurrence. Similarly, other studies have pointed to a desynchronization in striatal-frontal connectivity (Leaver et al., 2016), synergistic functional decoupling in the reward network correlated with anhedonia (Gong et al., 2018), and increased FC fluctuations within thalamic and basal-ganglia networks (Long et al., 2020).

A desynchronization or decoupling of neural networks may likely be an indicator of the functional pathophysiology of MDD, extending to other networks such as the DMN and the visual-attention network. In fact Marchetti et al. (2012) initially proposed an imbalance between task-positive and task-negative elements of the DMN as a risk factor for depression recurrence. Later studies in MDD have pointed to altered neural networks and connections with and within the DMN (Li et al., 2020; Liu et al., 2017), as well as excessive fluctuations in FC in DMN (Long et al., 2020). Others have shown a persistent reduction of low-frequency fluctuations (representing intrinsic local neuronal activities) in the precuneus and posterior cingulate cortex, despite treatment or achieved remission (Wang et al., 2020)—regions considered the functional core of the DMN (Utevsky et al., 2014). Such a MDD-related disruption in network communication in the DMN has also recently been reported with respect to rich-club organization (the basis for long-range, high-capacity signaling; Liu et al., 2020). Dominance of DMN activity has been associated with MDD recurrence and related to rumination (Hamilton et al., 2011; Lythe et al., 2015). Similarly, in this study, we found increased recruitment (lifetime) of the DMN during a depressive state versus previous remission, reflecting perhaps the incremental nature of DMN dominance and a particular failure to control internally focused thoughts in recurrence.

Other studies also point to disrupted communication in or with visual-attention circuits. For example, stronger connectivity of attention regulation circuits to DMN has been implied to relate to better responsivity to internally generated self-relevant thoughts rather than outside stimuli (Knyazev et al., 2018). Stability of FC (vs. more frequent and rapid shifts) in visual-attention regions, such as the ACC, calcarine sulcus, and middle occipital gyrus has been shown to predict improvement in depressive symptoms in MDD (Li et al., 2021). Here, we also found that the visual-attention circuit was more likely to occur during a recurrence, compared to remission, which could represent attempts to regulate and overcome depressive phenomena in patients experiencing a recurrence.

Importantly, what we show with the results of the current study is that network reconfiguration takes place within individuals when they transition from a state of remission to a depressive episode. As

such, implementing dynamic connectivity approaches in clinical populations could give insight into changes that occur across time in individuals, especially during vulnerable periods (e.g., recurrence of a depressive episode). Future work should investigate how these neural measures could be used to improve recurrence prevention and what would be the optimal time to administer treatment. The finding of increased segregation of certain brain networks during a depressive episode might help to identify ways of improving flexibility and integration of the implicated networks. For example, electroconvulsive therapy has been shown to impact ventral striatum connectivity—a region deemed to be a key structure contributing to network desynchronization in MDD (Leaver et al., 2016). Identifying the source of the transition from integrated to more segregated neural states could, therefore, be used in the future as a target for tailoring interventions based on individualized risk assessments.

## 4.1 | Interpretational issues

Several limitations should be considered with respect to the results of this study. Arguably, the reliability and generalizability of the presented inferences is limited by the low sample size (overall  $n = 28$ ; recurrent  $n = 11$ ). However, this should be weighed against the uniqueness and specificity of the sample—antidepressant-free patients with at least two past episodes of MDD, scanned during remission, followed-up, and then scanned again while in a depressive episode, as well as a matched comparison group of MDD participants without a recurrence when scanned again. While these findings should be taken tentatively and replicated in future longitudinal studies, they provide an initial insight into the neural biomarkers changing in the perspective of recurrence.

Although the nonrecurrent patients were in remission during the follow-up scan, a possibility remains that they had a depressive episode at a later time. The fact that we find differences in PL-state profiles in the recurring, but not in the nonrecurring group, is associated with the present experience of acute depressive symptoms. A full factorial comparison of recurrent and non-recurrent patients at baseline (and changes over time) was not possible given the group sample sizes. It is, therefore, not possible to draw direct conclusions with respect to differences between the two groups. Especially changes in DMN should be treated with caution and replicated in future studies given weak Bayesian evidence supporting null effects in this network in the nonrecurring group. Additionally, future investigations may identify how specific symptomatology, such as anhedonia (Servaes et al., 2017) relates to changes in these FC dynamics.

It could be argued that the networks we identified could be restricted due to the number of states ( $k$ ) that best represents FC dynamics. Here, we assessed our results for a wide range of  $k$  (from 2 to 20), and further demonstrated the consistency and significance of our findings across several choices of  $k$ . Although it can be argued that the networks were constrained by the parcellation atlas that was used - in contrast to Figueroa et al. (2019) who used the Anatomical

Automated Labeling atlas - we used a clinically relevant, custom-made “DBS80” parcellation, designed specifically for DBS studies.

Although the new “decoupling metric” was implemented based on results obtained from LEiDA, these two approaches provide novel insights regarding underlying differences in fractional occupancy of the reward network. As such, the decoupling metric is not only a confirmation, but also an extension of the results obtained using LEiDA. With LEiDA, only the epochs when a particular pattern is dominant (“represented by the leading” eigenvector) are taken into account, whereas decoupling is computed over the entire time series. This approach relies on the hypothesis that phase relationships between areas are critical. For example, one area consistently activates a bit later than the other—as such these areas would be coupled, but not in-phase, as typically captured by co-activation measures. Using this new metric, we can quantify the mean phase shift (or angular difference) between baseline and follow-up and, therefore, investigate whether depression recurrence is associated with a consistent dephasing of one network from the rest of the brain.

## 5 | CONCLUSION

With a unique repeated measures design of remitted depressed patients followed-up for 2.5 years while scanned in remission and in a recurrence episode, this study provides initial evidence of alterations in the brain's dynamical repertoire that may be associated with the transition from remission to recurrence of a depressive episode. These results highlight the potential role of widespread reconfiguration of networks known to be implicated in MDD, such as the DMN, reward, and attention circuits. Crucially, we show that these changes occur within individuals and as such provide a promising avenue for emerging personalized treatment.

### AFFILIATIONS

<sup>1</sup>Department of Biomedical Sciences of Cells and Systems, Cognitive Neuroscience Center, University Medical Center Groningen, University of Groningen, Groningen, the Netherlands

<sup>2</sup>Department of Clinical Medicine, Center for Functionally Integrative Neuroscience, Aarhus University, Aarhus, Denmark

<sup>3</sup>Department of Psychiatry, Radboud University Medical Centre, Nijmegen, the Netherlands

<sup>4</sup>Donders Institute for Brain, Cognition and Behavior, Radboud University, Nijmegen, the Netherlands

<sup>5</sup>Depression Expertise Center, ProPersona Mental Health Care, Nijmegen, the Netherlands

<sup>6</sup>Overwaal Centre of Expertise for Anxiety Disorders, OCD and PTSD, Pro Persona Mental Health Care, Nijmegen, the Netherlands

<sup>7</sup>Department of Psychiatry, Amsterdam UMC, Location AMC, Amsterdam, the Netherlands

<sup>8</sup>Department of Psychiatry, University Medical Centre Utrecht, Utrecht, the Netherlands

<sup>9</sup>School of Social Welfare, University of California, Berkeley, California, USA

<sup>10</sup>Department of Information and Communication Technologies, Center for Brain and Cognition, Computational Neuroscience Group, Universitat Pompeu Fabra, Barcelona, Spain

<sup>11</sup>Institució Catalana de la Recerca i Estudis Avançats (ICREA), Barcelona, Spain

<sup>12</sup>Centre for Eudaimonia and Human Flourishing, Linacre College, University of Oxford, Oxford, UK

<sup>13</sup>Center for Music in the Brain, Aarhus University, Aarhus, Denmark

<sup>14</sup>Department of Psychiatry, University of Oxford, Oxford, UK

<sup>15</sup>Life and Health Sciences Research Institute (ICVS), School of Medicine, University of Minho, Braga, Portugal

### ACKNOWLEDGMENTS

The DELTA-neuroimaging study was funded by the Dutch Brain Foundation (Hersenstichting; Grant #2009(2)-72). Further support was obtained by unrestricted personal grants from the AMC to Roel J. T. Mocking (AMC PhD Scholarship) and Caroline A. Figueroa (AMC MD-PhD Scholarship). Henricus G. Ruhé is supported by a NWO/ZonMW VENI-grant (#016.126.059). Anna Tyborowska and Nessa Ikani are partly funded by the Dutch Brain Foundation [Hersenstichting; Grant #HA2015.01.07; SMARD]. Roel J. T. Mocking is supported by an unrestricted ABC Talent Grant, unrestricted ZonMw GGZ fellowship, and Amsterdam UMC Starter Grant. Morten L. Kringelbach is supported by the Center for Music in the Brain, funded by the Danish National Research Foundation (DNRF117), and Centre for Eudaimonia and Human Flourishing at Linacre College funded by the Pettit and Carlsberg Foundations. Joana Cabral is supported by La Caixa Foundation (LCF/BQ/PR22/11920014) and the Portuguese Foundation for Science and Technology (UIDB/50026/2020, UIDP/50026/2020).

### CONFLICT OF INTEREST STATEMENT

The authors declare no conflicts of interest.

### DATA AVAILABILITY STATEMENT

Data is available upon request via the Donders Repository (<https://data.donders.ru.nl/>). Data can be provided by the Donders Institute for Brain, Cognition, and Behaviour pending scientific review and a completed data transfer agreement in collaboration with AmsterdamUMC. Requests for the data should be submitted to Henricus G. Ruhé. The MATLAB scripts used to analyse the data in this study are publicly available at <https://github.com/sonsolesalonsomartinez/rrMDD>.

### ORCID

Sonsoles Alonso  <https://orcid.org/0000-0001-9631-6664>

Anna Tyborowska  <https://orcid.org/0000-0002-7621-3497>

Nessa Ikani  <https://orcid.org/0000-0002-4466-5421>

Roel J. T. Mocking  <https://orcid.org/0000-0003-3543-3810>

Caroline A. Figueroa  <https://orcid.org/0000-0003-0692-2244>

Gustavo Deco  <https://orcid.org/0000-0002-8995-7583>

Morten L. Kringelbach  <https://orcid.org/0000-0002-3908-6898>

Joana Cabral  <https://orcid.org/0000-0002-6715-0826>

Henricus G. Ruhé  <https://orcid.org/0000-0001-6072-0358>

## REFERENCES

- Adrián-Ventura, J., Costumero, V., Parcet, M. A., & Ávila, C. (2019). Reward network connectivity "at rest" is associated with reward sensitivity in healthy adults: A resting-state fMRI study. *Cognitive, Affective and Behavioral Neuroscience*, 3(19), 726–736. <https://doi.org/10.3758/s13415-019-00688-1>
- Alonso Martínez, S., Deco, G., Ter Horst, G. J., & Cabral, J. (2020). The dynamics of functional brain networks associated with depressive symptoms in a nonclinical sample. *Frontiers in Neural Circuits*, 14, 570583. <https://doi.org/10.3389/fncir.2020.570583>
- Andersson, J. L. R., Jenkinson, M., & Smith, S. (2007). *Non-linear registration aka spatial normalisation*. FMRIB Technical Report TRO7JA2.
- Barrett, L. F., & Satpute, A. B. (2013). Large-scale brain networks in affective and social neuroscience: Towards an integrative functional architecture of the brain. *Current Opinion in Neurobiology*, 23, 361–372. <https://doi.org/10.1016/j.conb.2012.12.012>
- Benjamini, Y., & Hochberg, Y. (1995). Controlling the false discovery rate: A practical and powerful approach to multiple testing. *Journal of the Royal Statistical Society. Series B (Methodological)*, 57(1), 289–300.
- Blank, T. S., Meyer, B. M., Rabl, U., Schögl, P., Wieser, M. K., & Pezawas, L. (2021). Neurobiological predictors for clinical trajectories in fully remitted depressed patients. *Depression and Anxiety*, 38(4), 447–455. <https://doi.org/10.1002/da.23108>
- Bockting, C. L. H., Spinhoven, P., Wouters, L. F., Koeter, M. W. J., & Schene, A. H. (2009). Long-term effects of preventive cognitive therapy in recurrent depression: A 5.5-year follow-up study. *Journal of Clinical Psychiatry*, 70, 1621–1628. <https://doi.org/10.4088/JCP.08m04784blu>
- Bressler, S. L., & Menon, V. (2010). Large-scale brain networks in cognition: Emerging methods and principles. *Trends in Cognitive Sciences*, 14, 277–290. <https://doi.org/10.1016/j.tics.2010.04.004>
- Caballero-Gaudes, C., & Reynolds, R. C. (2017). Methods for cleaning the BOLD fMRI signal. *NeuroImage*, 154, 128–149. <https://doi.org/10.1016/j.neuroimage.2016.12.018>
- Cabral, J., Kringelbach, M. L., & Deco, G. (2017). Functional connectivity dynamically evolves on multiple time-scales over a static structural connectome: Models and mechanisms. *NeuroImage*, 160, 84–96. <https://doi.org/10.1016/j.neuroimage.2017.03.045>
- Connolly, C. G., Wu, J., Ho, T. C., Hoefft, F., Wolkowitz, O., Eisendrath, S., Frank, G., HENDREN, R., Max, J. E., Paulus, M. P., Tapert, S. F., Banerjee, D., Simmons, A. N., & Yang, T. T. (2013). Resting-state functional connectivity of subgenual anterior cingulate cortex in depressed adolescents. *Biological Psychiatry*, 74(12), 898–907. <https://doi.org/10.1016/j.biopsych.2013.05.036>
- Davey, C. G., Harrison, B. J., Yücel, M., & Allen, N. B. (2012). Regionally specific alterations in functional connectivity of the anterior cingulate cortex in major depressive disorder. *Psychological Medicine*, 42, 2071–2081. <https://doi.org/10.1017/S0033291712000323>
- Deco, G., & Kringelbach, M. L. (2014). Great expectations: Using whole-brain computational connectomics for understanding neuropsychiatric disorders. *Neuron*, 84(5), 892–905. <https://doi.org/10.1016/j.neuron.2014.08.034>
- Deco, G., Tononi, G., Boly, M., & Kringelbach, M. L. (2015). Rethinking segregation and integration: Contributions of whole-brain modelling. *Nature Reviews Neuroscience*, 16, 430–439. <https://doi.org/10.1038/nrn3963>
- Deco, G., Vidaurre, F., & Kringelbach, M. (2021). Revisiting the global workspace orchestrating the hierarchical organization of the human brain. *Nature Human Behaviour*, 5, 497–511. <https://doi.org/10.1038/s41562-020-01003-6>
- Desikan, R. S., Ségonne, F., Fischl, B., Quinn, B. T., Dickerson, B. C., Blacker, D., Buckner, R. L., Dale, A. M., Maguire, R. P., Hyman, B. T., Albert, M. S., & Killiany, R. J. (2006). An automated labeling system for subdividing the human cerebral cortex on MRI scans into gyral based regions of interest. *NeuroImage*, 31(3), 968–980. <https://doi.org/10.1016/j.neuroimage.2006.01.021>
- Etkin, A., Egner, T., & Kalisch, R. (2011). Emotional processing in anterior cingulate and medial prefrontal cortex. *Trends in Cognitive Sciences*, 15(2), 85–93. <https://doi.org/10.1016/j.tics.2010.11.004>
- Farinha, M., Amado, C., Morgado, P., & Cabral, J. (2022). Increased excursions to functional networks in schizophrenia in the absence of task. *Frontiers in Neuroscience*, 16, 821179.
- Figuroa, C. A., Cabral, J., Mocking, R. J. T., Rapuano, K. M., van Hartevelt, T. J., Deco, G., Expert, P., Schene, A. H., Kringelbach, M. L., & Ruhé, H. G. (2019). Altered ability to access a clinically relevant control network in patients remitted from major depressive disorder. *Human Brain Mapping*, 40(9), 2771–2786. <https://doi.org/10.1002/hbm.24559>
- Friston, K. J., Williams, S., Howard, R., Frackowiak, R. S. J., & Turner, R. (1996). Movement-related effects in fMRI time-series. *Magnetic Resonance in Medicine*, 35, 346–355. <https://doi.org/10.1002/mrm.1910350312>
- Gao, Q., Zou, K., He, Z., Sun, X., & Chen, H. (2016). Causal connectivity alterations of cortical-subcortical circuit anchored on reduced hemodynamic response brain regions in first-episode drug-naïve major depressive disorder. *Scientific Reports*, 6, 1–12. <https://doi.org/10.1038/srep21861>
- Geugies, H., Mocking, R. J. T., Figuroa, C. A., Groot, P. F. C., Marsman, J. C., Servaas, M. N., Steele, J. D., Schene, A. H., & Ruhé, H. G. (2019). Impaired reward-related learning signals in remitted unmedicated patients with recurrent depression. *Brain*, 142, 2510–2522. <https://doi.org/10.1093/brain/awz214>
- Gong, L., He, C., Zhang, H., Zhang, H., Zhang, Z., & Xie, C. (2018). Disrupted reward and cognitive control networks contribute to anhedonia in depression. *Journal of Psychiatric Research*, 103(338), 61–68. <https://doi.org/10.1016/j.jpsychires.2018.05.010>
- Gradin, V. B., Kumar, P., Waiter, G., Ahearn, T., Stickle, C., Milders, M., Reid, I., Hall, J., & Steele, J. D. (2011). Expected value and prediction error abnormalities in depression and schizophrenia. *Brain*, 134, 1751–1764. <https://doi.org/10.1093/brain/awr059>
- Gray, J. P., Müller, V. I., Eickhoff, S. B., & Fox, P. T. (2020). Multimodal abnormalities of brain structure and function in major depressive disorder: A meta-analysis of neuroimaging studies. *American Journal of Psychiatry*, 177, 422–434. <https://doi.org/10.1176/appi.ajp.2019.19050560>
- Greve, D. N., & Fischl, B. (2009). Accurate and robust brain image alignment using boundary-based registration. *NeuroImage*, 48, 63–72. <https://doi.org/10.1016/j.neuroimage.2009.06.060>
- Haber, S., & Knudson, B. (2010). The reward circuit: Linking primate anatomy and human imaging. *Neuropsychopharmacology*, 35(1), 4–26. <https://doi.org/10.1038/npp.2009.129>
- Hall, G. B. C., Milne, A. M. B., & MacQueen, G. M. (2014). An fMRI study of reward circuitry in patients with minimal or extensive history of major depression. *European Archives of Psychiatry and Clinical Neuroscience*, 264, 187–198. <https://doi.org/10.1007/s00406-013-0437-9>
- Hamilton, J. P., Chen, M. C., & Gotlib, I. H. (2013). Neural systems approaches to understanding major depressive disorder: An intrinsic functional organization perspective. *Neurobiology of Disease*, 52, 4–11. <https://doi.org/10.1016/j.nbd.2012.01.015>
- Hamilton, J. P., Furman, D. J., Chang, C., Thomason, M. E., Dennis, E., & Gotlib, I. H. (2011). Default-mode and task-positive network activity in major depressive disorder: Implications for adaptive and maladaptive rumination. *Biological Psychiatry*, 70(4), 327–333. <https://doi.org/10.1016/j.biopsych.2011.02.003.Default-mode>



- Hancock, F., Cabral, J., Luppi, A., Rosas, F., Mediano, P., Dipasquale, O., & Turkheimer, F. (2022). Metastability, fractal scaling, and synergistic information processing: What phase relationships reveal about intrinsic brain activity. *NeuroImage*, 259, 119433. <https://doi.org/10.1016/j.neuroimage.2022.119433>
- Hardeveld, F., Spijker, J., De Graaf, R., Nolen, W. A., & Beekman, A. T. F. (2010). Prevalence and predictors of recurrence of major depressive disorder in the adult population. *Acta Psychiatrica Scandinavica*, 122, 184–191. <https://doi.org/10.1111/j.1600-0447.2009.01519.x>
- Institute of Health Metrics and Evaluation. (2019). Global Health Data Exchange (GHDx). <https://vizhub.healthdata.org/gbd-results/>
- Jenkinson, M., Bannister, P., Brady, M., & Smith, S. (2002). Improved optimization for the robust and accurate linear registration and motion correction of brain images. *NeuroImage*, 17, 825–841. [https://doi.org/10.1016/S1053-8119\(02\)91132-8](https://doi.org/10.1016/S1053-8119(02)91132-8)
- Jenkinson, M., & Smith, S. (2001). A global optimisation method for robust affine registration of brain images. *Medical Image Analysis*, 5, 143–156. [https://doi.org/10.1016/S1361-8415\(01\)00036-6](https://doi.org/10.1016/S1361-8415(01)00036-6)
- Kaiser, R., Whitfield-Gabrieli, S., Dillon, D. G., Goer, F., Beltzer, M., Minkel, J., Smoski, M., Dichter, G., & Pizzagalli, D. A. (2016). Dynamic resting-state functional connectivity in major depression. *Neuropsychopharmacology*, 41, 1822–1830. <https://doi.org/10.1038/npp.2015.352>
- Kaiser, R. H., Andrews-Hanna, J. R., Wager, T. D., & Pizzagalli, D. A. (2015). Large-scale network dysfunction in major depressive disorder: A meta-analysis of resting-state functional connectivity. *JAMA Psychiatry*, 72(6), 603–611. <https://doi.org/10.1001/jamapsychiatry.2015.0071>
- Kantrowitz, J. T., Dong, Z., Milak, M. S., Rashid, R., Kegeles, L. S., Javitt, D. C., Lieberman, J. A., & Mann, J. J. (2021). Ventromedial prefrontal cortex/anterior cingulate cortex Glx, glutamate, and GABA levels in medication-free major depressive disorder. *Translational Psychiatry*, 11, 419. <https://doi.org/10.1038/s41398-021-01541-1>
- Knyazev, G. G., Savostyanov, A. N., Bocharov, A. V., Brak, I. V., Osipov, E. A., Filimonova, E. A., Sapirigyn, A. E., & Aftanas, L. I. (2018). Task-positive and task-negative networks in major depressive disorder: A combined fMRI and EEG study. *Journal of Affective Disorders*, 235, 211–219. <https://doi.org/10.1016/j.jad.2018.04.003>
- Kringelbach, M. L., & Deco, G. (2020). Brain states and transitions: Insights from computational neuroscience. *Cell Reports*, 32(10), 108128. <https://doi.org/10.1016/j.celrep.2020.108128>
- Kumar, P., Waiter, G., Milders, M., Reid, I., & Steele, J. D. (2008). Abnormal temporal difference reward-learning signals in major depression. *Brain*, 131, 2084–2093. <https://doi.org/10.1093/brain/awn136>
- Larabi, D. I., Renken, R. J., Cabral, J., Marsman, J. B. C., Aleman, A., & Ćurčić-Blake, B. (2020). Trait self-reflectiveness relates to time-varying dynamics of resting state functional connectivity and underlying structural connectomes: Role of the default mode network. *NeuroImage*, 219, 116896. <https://doi.org/10.1016/j.neuroimage.2020.116896>
- Leaver, A. M., Espinoza, R., Joshi, S. H., Vasavada, M., Njau, S., Woods, R. P., & Narr, K. L. (2016). Desynchronization and plasticity of striato-frontal connectivity in major depressive disorder. *Cerebral Cortex*, 26, 4337–4346. <https://doi.org/10.1093/cercor/bhv207>
- Li, B., Friston, K., Mody, M., & Hu, H. L. D. (2018). A brain network model for depression: From symptom understanding to disease intervention. *CNS Neuroscience & Therapeutics*, 24(11), 1004–1019. <https://doi.org/10.1111/cns.12998>
- Li, G., Liu, Y., Zheng, Y., Li, D., Liang, X., Chen, Y., Cui, Y., Yap, P.-T., Qiu, S., Zhang, H., & Shen, D. (2020). Large-scale dynamic causal modeling of major depressive disorder based on resting-state functional magnetic resonance imaging. *Human Brain Mapping*, 41(4), 865–881. <https://doi.org/10.1002/hbm.24845>
- Li, X., Zhang, Y., Meng, C., Zhang, C., Zhao, W., Zhu, D., Zhu, D. M., & Zhu, J. (2021). Functional stability predicts depressive and cognitive improvement in major depressive disorder: A longitudinal functional MRI study. *Progress in Neuro-Psychopharmacology and Biological Psychiatry*, 111, 110396. <https://doi.org/10.1016/j.pnpbp.2021.110396>
- Liu, C. H., Ma, X., Yuan, Z., Song, L. P., Jing, B., Lu, H. Y., Tang, L.-R., Fan, J., Walter, M., Liu, C.-Z., Wang, L., & Wang, C. Y. (2017). Decreased resting-state activity in the precuneus is associated with depressive episodes in recurrent depression. *Journal of Clinical Psychiatry*, 78, e372–e382. <https://doi.org/10.4088/JCP.15m10022>
- Liu, J., Fan, Y., Zeng, L., Liu, B., Ju, Y., Wang, M., Dong, Q., Lu, X., Sun, J., Zhang, L., Guo, H., Zhao, F., Li, W., Zhang, L., Li, Z., Liao, M., Zhang, Y., Hu, D., & Li, L. (2021). The neuroprogressive nature of major depressive disorder: Evidence from an intrinsic connectome analysis. *Translational Psychiatry*, 11(1), 102. <https://doi.org/10.1038/s41398-021-01227-8>
- Liu, X., He, C., Fan, D., Zhu, Y., Zang, F., Wang, Q., Zhang, H., Zhang, Z., Zhang, H., & Xie, C. (2020). Disrupted rich-club network organization and individualized identification of patients with major depressive disorder. *Progress in Neuro-psychopharmacology & Biological Psychiatry*, 108, 110074. <https://doi.org/10.1016/j.pnpbp.2020.110074>
- Long, Y., Cao, H., Yan, C., Chen, X., Li, L., Castellanos, F. X., Bai, T., Bo, Q., Chen, G., Chen, N., Chen, W., Cheng, C., Cheng, Y., Cui, X., Duan, J., Fang, Y., Gong, Q., Guo, W., Hou, Z., ... Liu, Z. (2020). Altered resting-state dynamic functional brain networks in major depressive disorder: Findings from the REST-meta-MDD consortium. *NeuroImage: Clinical*, 26, 102163. <https://doi.org/10.1016/j.nicl.2020.102163>
- Lythe, K. E., Moll, J., Gethin, J. A., Workman, C. I., Green, S., Ralph, M. A. L., Deakin, J. F. W., & Zahn, R. (2015). Self-blame-selective hyperconnectivity between anterior temporal and subgenual cortices and prediction of recurrent depressive episodes. *JAMA Psychiatry*, 72, 1119–1126. <https://doi.org/10.1001/jamapsychiatry.2015.1813>
- Marchetti, I., Koster, E. H. W., Sonuga-Barke, E. J., & De Raedt, R. (2012). The default mode network and recurrent depression: A neurobiological model of cognitive risk factors. *Neuropsychology Review*, 22, 229–251. <https://doi.org/10.1007/s11065-012-9199-9>
- Martin-Soelch, C. (2009). Is depression associated with dysfunction of the central reward system? *Biochemical Society Transactions*, 37, 313–317. <https://doi.org/10.1042/BST0370313>
- Menon, V. (2011). Large-scale brain networks and psychopathology: A unifying triple network model. *Trends in Cognitive Sciences*, 15(10), 483–506. <https://doi.org/10.1016/j.tics.2011.08.003>
- Mocking, R. J. T., Figueroa, C. A., Rive, M. M., Geugies, H., Servaas, M. N., Assies, J., Koeter, M. W. J., Vaz, F. M., Wichers, M., van Straalen, J. P., de Raedt, R., Bockting, C. L. H., Harmer, C. J., Schene, A. H., & Ruhé, H. G. (2016). Vulnerability for new episodes in recurrent major depressive disorder: Protocol for the longitudinal delta-neuroimaging cohort study. *BMJ Open*, 6(3), 1–17. <https://doi.org/10.1136/bmjopen-2015-009510>
- Mulders, P. C., van Eijndhoven, P. F., Schene, A. H., Beckmann, C. F., & Tendolkar, I. (2015). Resting-state functional connectivity in major depressive disorder: A review. *Neuroscience and Biobehavioral Reviews*, 56, 330–344. <https://doi.org/10.1016/j.neubiorev.2015.07.014>
- Pizzagalli, D. A., Holmes, A. J., Dillon, D. G., Goetz, E. L., Birk, J. L., Bogdan, R., Dougherty, D. D., Iosifescu, D. V., Rauch, S. L., & Fava, M. (2009). Reduced caudate and nucleus accumbens response to rewards in unmedicated individuals with major depressive disorder. *American Journal of Psychiatry*, 166, 702–710. <https://doi.org/10.1176/appi.ajp.2008.08081201>
- Pruim, R. H. R., Mennes, M., van Rooij, D., Llera, A., Buitelaar, J. K., & Beckmann, C. F. (2015). ICA-AROMA: A robust ICA-based strategy for removing motion artifacts from fMRI data. *NeuroImage*, 112, 267–277. <https://doi.org/10.1016/j.neuroimage.2015.02.064>
- Rive, M. M., van Rooijen, G., Veltman, D. J., Phillips, M. L., Schene, A. H., & Ruhé, H. G. (2013). Neural correlates of dysfunctional emotion regulation in major depressive disorder. A systematic review of



- neuroimaging studies. *Neuroscience Biobehavioral Reviews*, 37, 2529–2553. <https://doi.org/10.1016/j.neubiorev.2013.07.018>
- Robinson, O. J., Cools, R., Carlisi, C. O., Sahakian, B. J., & Drevets, W. C. (2012). Ventral striatum response during reward and punishment reversal learning in unmedicated major depressive disorder. *American Journal of Psychiatry*, 169, 152–159. <https://doi.org/10.1176/appi.ajp.2011.11010137>
- Ruhé, H. G., Mocking, R. J. T., Figueroa, C. A., Seeverens, P. W. J., Ikani, N., Tyborowska, A., Browning, M., Vrijisen, J. N., Harmer, C. J., & Schene, A. H. (2019). Emotional biases and recurrence in major depressive disorder. Results of 2.5 years follow-up of drug-free cohort vulnerable for recurrence. *Frontiers in Psychiatry*, 10, 1–18. <https://doi.org/10.3389/fpsy.2019.00145>
- Satterthwaite, T. D., Kable, J. W., Vandekar, L., Katchmar, N., Bassett, D. S., Baldassano, C. F., Ruparel, K., Elliott, M. A., Sheline, Y. I., Gur, R. C., Gur, R. E., Davatzikos, C., Leibenluft, E., Thase, M. E., & Wolf, D. H. (2015). Common and dissociable dysfunction of the reward system in bipolar and unipolar depression. *Neuropsychopharmacology*, 40, 2258–2268. <https://doi.org/10.1038/npp.2015.75>
- Schott, B., Minuzzi, L., Krebs, R., Elmenhorst, D., Lang, M., Winz, O., Seidenbecher, C., Coenen, H., Heinze, H., Zilles, K., Düzal, E., & Bauer, A. (2008). Mesolimbic functional magnetic resonance imaging activations during reward anticipation correlate with reward-related ventral striatal dopamine release. *Journal of Neuroscience*, 28(5), 14311–14319. <https://doi.org/10.1523/JNEUROSCI.2058-08.2008>
- Servaas, M. N., Riese, H., Renken, R. J., Wichers, M., Bastiaansen, J. A., Figueroa, C. A., Geugies, H., Mocking, R. J., Geerligs, L., Marsman, J.-B. C., Aleman, A., Schene, A. H., Schoevers, R. A., & Ruhé, H. G. (2017). Associations between daily affective instability and connectomics in functional subnetworks in remitted patients with recurrent major depressive disorder. *Neuropsychopharmacology*, 42, 2583–2592. <https://doi.org/10.1038/npp.2017.65>
- Smoski, M. J., Felder, J., Bizzell, J., Green, S. R., Ernst, M., Lynch, T. R., & Dichter, G. S. (2009). fMRI of alterations in reward selection, anticipation, and feedback in major depressive disorder. *Journal of Affective Disorders*, 118(1–3), 69–78. <https://doi.org/10.1016/j.jad.2009.01.034>
- Stark, E. A., Cabral, J., Riem, M. M. E., Van IJzendoorn, M. H., Stein, A., & Kringelbach, M. L. (2020). The power of smiling: The adult brain networks underlying learned infant emotionality. *Cerebral Cortex*, 30(4), 2019–2029. <https://doi.org/10.1093/cercor/bhz219>
- Utevsky, A. V., Smith, D. V., & Huettel, S. A. (2014). Precuneus is a functional core of the default-mode network. *Journal of Neuroscience*, 34(3), 932–940. <https://doi.org/10.1523/JNEUROSCI.4227-13.2014>
- van Tol, M., Veer, I. M., van der Wee, N. J. A., Aleman, A., van Buchem, M. A., Rombouts, S. A. R. B., & Johnstone, T. (2013). Whole-brain functional connectivity during emotional word classification in medication-free major depressive disorder: Abnormal salience circuitry and relations to positive emotionality. *NeuroImage: Clinical*, 2, 790–796. <https://doi.org/10.1016/j.nicl.2013.05.012>
- Wang, M., Ju, Y., Lu, X., Sun, J., Dong, Q., Liu, J., Zhang, L., Zhang, Y., Zhang, S., Wang, Z., Liu, B., & Li, L. (2020). Longitudinal changes of amplitude of low-frequency fluctuations in MDD patients: A 6-month follow-up resting-state functional magnetic resonance imaging study. *Journal of Affective Disorders*, 276, 411–417. <https://doi.org/10.1016/j.jad.2020.07.067>
- Wong, W., Cabral, J., Rane, R., Ly, R., Kringelbach, M. L., & Feusner, J. D. (2021). Effects of visual attention modulation on dynamic functional connectivity during own-face viewing in body dysmorphic disorder. *Neuropsychopharmacology*, 46(11), 2030–2038. <https://doi.org/10.1038/s41386-021-01039-w>
- Yarkoni, T., Poldrack, R. A., Nichols, T. E., Van Essen, D. C., & Wager, T. D. (2011). Large-scale automated synthesis of human functional neuroimaging data. *Nature Methods*, 8, 665–670. <https://doi.org/10.1038/nmeth.1635>
- Zheng, H., Li, F., Bo, Q., Li, X., Yao, Z., Wang, C., & Wu, X. (2018). The dynamic characteristics of the anterior cingulate cortex in resting-state fMRI of patients with depression. *Journal of Affective Disorders*, 227, 391–391. <https://doi.org/10.1016/j.jad.2017.11.026>
- Zhu, X., Helpman, L., Papini, S., Schneier, F., Markowitz, J. C., van Meter, P. E., Lindquist, M. A., Wager, T. D., & Neria, Y. (2017). Altered resting state functional connectivity of fear and reward circuitry in comorbid PTSD and major depression. *Depression and Anxiety*, 34(7), 641–650. <https://doi.org/10.1002/da.22594>

## SUPPORTING INFORMATION

Additional supporting information can be found online in the Supporting Information section at the end of this article.

**How to cite this article:** Alonso, S., Tyborowska, A., Ikani, N., Mocking, R. J. T., Figueroa, C. A., Schene, A. H., Deco, G., Kringelbach, M. L., Cabral, J., & Ruhé, H. G. (2023). Depression recurrence is accompanied by longer periods in default mode and more frequent attentional and reward processing dynamic brain-states during resting-state activity. *Human Brain Mapping*, 44(17), 5770–5783. <https://doi.org/10.1002/hbm.26475>